Journal for
ImmunoTherapy of Cancer

MDSCs-derived GPR84 induces CD8+ T-cell senescence via p53 activation to suppress the antitumor response

Jinyan Liu,[1] Jiayin Liu,[1,2] Guohui Qin,[1] Jiahui Li,[1] Ziyi Fu,[1,2] Jieyao Li,[3] Miaomiao Li,[1] Caijuan Guo,[1] Ming Zhao,[1] Zhen Zhang,[1] Feng Li ![ORCID],[1] Xuan Zhao,[1] Liping Wang,[3] Yi Zhang ![ORCID] [1,3,4]

[1]Biotherapy Center and Cancer Center, The First Affiliated Hospital of Zhengzhou University, Zhengzhou, Henan, China
[2]School of Life Sciences, Zhengzhou University, Zhengzhou, Henan, China
[3]Department of Oncology, The First Affiliated Hospital of Zhengzhou University, Zhengzhou, Henan, China
[4]State Key Laboratory of Esophageal Cancer Prevention & and Treatment, Zhengzhou, Henan, China

Correspondence to
Professor Yi Zhang;
yizhang@zzu.edu.cn

ABSTRACT

Backgrounds G-protein-coupled receptor 84 (GPR84) marks a subset of myeloid-derived suppressor cells (MDSCs) with stronger immunosuppression in the tumor microenvironment. Yet, how GPR84 endowed the stronger inhibition of MDSCs to CD8+ T cells function is not well established. In this study, we aimed to identify the underlying mechanism behind the immunosuppression of CD8+ T cells by GPR84+ MDSCs.

Methods The role and underlying mechanism that MDSCs or exosomes (Exo) regulates the function of CD8+ T cells were investigated using immunofluorescence, fluorescence activating cell sorter (FACS), quantitative real-time PCR, western blot, ELISA, Confocal, RNA-sequencing (RNA-seq), etc. In vivo efficacy and mechanistic studies were conducted with wild type, GPR84 and p53 knockout C57/BL6 mice.

Results Here, we showed that the transfer of GPR84 from MDSCs to CD8+ T cells via the Exo attenuated the antitumor response. This inhibitory effect was also observed in GPR84-overexpressed CD8+ T cells, whereas depleting GPR84 elevated CD8+ T cells proliferation and function in vitro and in vivo. RNA-seq analysis of CD8+ T cells demonstrated the activation of the p53 signaling pathway in CD8+ T cells treated with GPR84+ MDSCs culture medium. While knockout p53 did not induce senescence in CD8+ T cells treated with GPR84+ MDSCs. The per cent of GPR84+ CD8+ T cells work as a negative indicator for patients' prognosis and response to chemotherapy.

Conclusions These data demonstrated that the transfer of GPR84 from MDSCs to CD8+ T cells induces T-cell senescence via the p53 signaling pathway, which could explain the strong immunosuppression of GPR84 endowed to MDSCs.

INTRODUCTION

Myeloid-derived suppressor cells (MDSCs) are a heterogeneous population of suppressive innate immune cells, including immature and highly immune-suppressive monocytic and granulocytic lineage cells in mice and humans.[1] The accumulation of MDSCs in the tumor microenvironment (TME) impedes T-cell mediated antitumor response, and further induces cancer progression and clinical

WHAT IS ALREADY KNOWN ON THIS TOPIC

⇒ Our previous study reported that G-protein-coupled receptor 84 (GPR84) marks a subpopulation of myeloid-derived suppressor cells (MDSCs) with stronger immunosuppression. However, why and how GPR84+ MDSCs exhibited enhanced inhibition on CD8+ T cells function remains elusive.

WHAT THIS STUDY ADDS

⇒ Herein, we observed that GPR84 could be transferred from MDSCs to CD8+ T cells to inhibit CD8+ T cells function in the exosome way, and blocking exosome secretion reversed the CD8+ T cells function. Mechanistically, GPR84 transferred on CD8+ T cells activated the p53 pathway to induce senescence. Moreover, we validated the negative indicator of GPR84 on CD8+ T cells function, chemotherapy response and prognosis, indicating the significance of GPR84 blockade in the tumor microenvironment.

HOW THIS STUDY MIGHT AFFECT RESEARCH, PRACTICE OR POLICY

⇒ The transfer of GPR84 from MDSCs to CD8+ T cells in the tumor microenvironment suppresses antitumor ability and negatively affects patients' response to chemotherapeutic treatment, indicating the significance of developing a GPR84 antagonist for cancer treatment.

treatment failure.[2] Identification of key molecule(s) involved in the MDSCs function will be required to target eliminate MDSCs to liberate the antitumor ability of cytotoxic T cells and to boost cancer immunotherapy efficacy. Several markers have been identified as the major regulators in MDSCs function, such as general control nonderepressible 2 (GCN2),[3] β2-adrenergic receptor[4] and the triggering receptor expressed on myeloid cell 1.[5] Previously, our group reported that G-protein-coupled receptor 84 (GPR84), a member of the G-protein coupled receptor (GPCR) superfamily, marks a subset of stronger immunosuppressive

MDSCs than those lacking GPR84, and blocking GPR84 could enhance the anti-programmed cell death-1 (PD-1) therapy efficacy.[6] However, how GPR84 endows higher immunosuppression to MDSCs to suppress CD8^{+} T-cell antitumor response remains unexplored. Therefore, we went on to investigate the underlying mechanism of GPR84 that drove stronger immunosuppression on MDSCs to CD8^{+} T cells in this study.

Multiple studies have been reported to reveal the interaction and underlying mechanisms between MDSCs and cytotoxic T cells inside the TME,[7] which could be summarized as direct interaction (such as FasL/Fas[8] and programmed cell death-ligand 1 (PD-L1)/PD-1[9]) and distant communication (such as secreting Arg1, iNOS, IL-10, exosomes).[2 10 11] Exosomes (Exos), an extracellular vesicle, are small (30 to 100 nm) membrane-bound particles containing a variety of molecules, and work as a major player in MDSCs induced cytotoxic T cells dysfunction.[12] MDSCs-Exos induced hyper-activating or exhausting CD8^{+} T cells and elevated reactive oxygen species (ROS) production to elicit activation-induced cell death in CD8^{+} T cells.[11] Other proteins enriched in MDSCs-Exos, such as PD-L1, mediate the antitumor function of CD8^{+} T cells.[11 13]

MDSCs suppressed CD8^{+} T cells function depending on inducing T cells exhaustion, dysfunction or senescence, with defective killing abilities in the TME.[14 15] CD8^{+} T cells senescence is characterized by increased β-galactosidase activity,[16] permanent loss of CD28 expression, altered cytokine profiles, upregulation of cell cycle-related genes (p53, p21, and p16), and various functional changes.[17] Several factors, including tumor-derived endogenous cyclic AMP,[18] tumor-derived metabolites,[19] elevated SMAD levels, and MDSCs,[20] have been reported to induce CD8^{+} T cells senescence in the TME. Oxidative stress caused by excess ROS induces DNA damage to cause T-cell senescence.[21]

As a series of research, in this study, we investigated the molecular changes and underlying mechanisms that occur in CD8^{+} T cells after interacting with GPR84^{+} MDSCs. By co-culturing GPR84^{+} MDSCs and CD8^{+} T cells directly or indirectly, we demonstrated the transfer of GPR84 from MDSCs to CD8^{+} T cells suppressed CD8^{+} T cells proliferation and reduced the cytotoxic cytokines production both in vitro and in vivo. Mechanistically, GPR84-containing Exo secreted by MDSCs was swallowed by CD8^{+} T cells, then the transferred GPR84 induced CD8^{+} T cells senescence via p53 pathway. Moreover, we observed higher GPR84^{+}CD8^{+} T cells were negatively correlated with patients with cancer survival and clinical treatment efficiency. Together with our previous research,[6] this study further reveals the underlying mechanism of GPR84^{+} MDSCs stronger immunosuppression to CD8^{+} T cells, which emphasizes the importance of GPR84 blockade in TME to suppress tumor progression and to enhance clinical treatment efficacy.

MATERIALS AND METHODS
Mice
Female C57BL/6J mice (6–8 weeks old) were purchased from the Beijing Charles River Company (Beijing, China). C57BL/6J–GPR84-deficient (GPR84^{−/−}) mice were provided by BRL+Medicine (Shanghai, China). To detect the GPR84 transgene in GPR84^{−/−} mice, genomic DNA was extracted from the toes of GPR84^{−/−} mice, and PCR analysis of the GPR84 transgene was performed using the following primer sequences: forward, 5′-GGAAGCTGCCAGGTTTATG-3′ and reverse, 5′-CCTGAATGGGAAAGTGGTG-3′. OT-1 mice were kindly provided by the Bo Huang lab at the Institute of Basic Medicine, Chinese Academy of Medical Sciences. These mice were crossed with GPR84-deficient mice to generate OT-1 GPR84^{−/−} mice. Six to eight weeks old mice were used for the experiments. Trp53^{−/−} mice were purchased from GemPharmatech. This study was approved by Ethics Committee of Zhengzhou University (zzu-LAC 20210702 (06)).

Cd8[+] T-cell isolation and culture in vitro
Spleen cells were harvested from experimental mice and subjected to magnet-activated cell sorting using a mouse CD8^{+} T Cell Isolation Kit (Miltenyi Biotec) according to the manufacturer's instructions. CD8^{+} T cells were cultured in vitro in a standard T-cell culture medium comprising Roswell Park Memorial Institute (RPMI) 1640 medium (Sigma), 10% fetal bovine serum (Sigma), 1% penicillin-streptomycin-glutamine, and interleukin (IL)-2. Unless otherwise indicated, cells were seeded at 2.5×10^6 cells per well in 12-well plates and stimulated with anti-CD3 (BioLegend) and anti-CD28 (BioLegend) for about 3 days. The cells were used for direct or co-incubation assays using flow cytometry.

Bone marrow cell isolation and MDSCs induction
Bone marrow cells were flushed from the tibias and fibulas of mice using sterile phosphate buffered saline (PBS). Red blood cells were lysed for 7 min at room temperature (RT, 25°C) using Red Cell Lysis Buffer, washed with RPMI 1640 medium, and then resuspended at 1×10^7 cells/mL with RPMI 1640 medium containing granulocyte colony-stimulating factor (G-CSF) (PeproTech) and GM-CSF (PeproTech), and incubated at 37°C (5% CO_2). The cells were obtained and analyzed by flow cytometry to examine the GPR84 level or for co-incubation assays.

In vitro co-culture assays
In vitro co-culture assays were performed using 48-well plates. CD8^{+} T cells and wild type or GPR84^{−/−} MDSCs were co-cultured at a ratio of 1:4 unless otherwise stated. In the indirect co-culture assay, MDSCs were cultured in the upper chamber and CD8^{+} T cells in the lower chamber of the transwell plate (pore size=0.4 μm). In the MDSCs-derived Exo secretion suppression assay, wild type or GPR84^{−/−} MDSCs were pretreated with GW4869 (MedChemExpress) for 2 hours and then co-cultured with

CD8$^+$ T cells. Also, CD8$^+$ T cells obtained from Trp53$^{-/-}$ mice were also used in the co-culture assays. The CD8$^+$ T cells were further analyzed by flow cytometry to detect GPR84 level, proliferation-related and function-related markers or senescence-associated-beta-galactosidase (SA-β-gal) staining.

T-cell proliferation and function assay
At the indicated time points, cells were collected and analyzed for cell proliferation through cell counting or Ki67 expression followed by flow cytometry. To assess T-cell cytokine production, CD8$^+$ T cells were stimulated with Phorbol-12-myristate-13-acetate (50 ng/mL) and ionomycin (500 ng/mL) in the presence of GolgiStop (4 µL per 6 mL culture) for 6 hours. Intracellular cytokine (IL-2, tumor necrosis factor (TNF)-α, and interferon (IFN)-γ) production was then analyzed using flow cytometry.

Exosome isolation and labeling
The MDSCs culture supernatant was centrifuged at 300×g for 10 min, 1,200×g for 20 min, and 10,000×g for 30 min at 4°C. The supernatant from the final centrifugation was filtered using a 0.22 µm filter and ultracentrifuged at 100,000×g for 1 hour at 4°C. The final pellets were resuspended in PBS. The particle size and morphology of the Exo were measured by transmission electron microscope (TEM) imaging. The amount of Exo protein recovered was measured using a BCA protein assay kit (Yeasen, Shanghai, China) and then was used for western blot. Exos were labeled with PKH67 (Sigma-Aldrich) according to the manufacturer's instructions for further assay.

Quantitative real-time PCR
Total RNA was isolated using TRIzol reagent (Invitrogen, Thermo Fisher Scientific) according to the manufacturer's instructions. Complementary DNA was prepared using a SuperScript III First-Strand Synthesis Supermix Kit (Invitrogen, Thermo Fisher Scientific). Quantitative real-time PCR (qPCR) was performed using the CFX96 qPCR system and SYBR Green PCR premix (Bio-Rad) according to the manufacturer's instructions. The primer sequences used were listed. GPR84: forward, 5′-TCTC ATTGCTCTAGGACGCTAC-3′ and reverse, 5′-AGAC AAAAACATTCCAGAGGGG-3′. All samples were normalized to GAPDH expression detected using the primers: forward, 5′-TGACCTCAACTACATGGTCTACA-3′ and reverse, 5′-CTTCCCATTCTCGGCCTTG-3′. The relative fold change was calculated using the $2^{-\Delta\Delta Ct}$ method.

Western blot analysis
Total protein was extracted using the radioimmunoprecipitation assay lysis buffer (Beyotime) and supplemented with a phosphatase inhibitor cocktail (Sigma) and protease inhibitor cocktail (Sigma) (following the manufacturers' instructions). Protein concentration was measured using a BCA assay kit (Thermo Fisher Scientific). Equal amounts of protein were resolved on a 12% SDS-PAGE gel and then transferred onto a nitrocellulose filter membrane (GEbio). The membrane was blocked with 5% bovine serum albumin (BSA) in tris buffered saline (TBST) and incubated with specific primary antibodies against GPR84 (Bioss), Tsg101 (Abcam), CD9 (Abcam), p53 (Abcam), p-p53 (Abcam), GAPDH (Abcam), β-Actin (Cell Signaling Technology (CST)). After incubation with secondary horseradish peroxidase (HRP)-conjugated goat anti-rabbit IgG (ZSBiO) (according to the manufacturer's protocol), the membranes were scanned using an enhanced chemiluminescent detection system.

Animal models
Wild type (WT) mice were inoculated subcutaneously with 5×10^5 B16-OVA melanoma cells in the right flank. Once the tumor size reached ~10 mm^2, CD8$^+$ T cells were isolated from spleens of OT-1 WT or GPR84$^{-/-}$ mice and stimulated with anti-CD3 and anti-CD28 antibodies in vitro for 24 hours. The following day, 1×10^7 CD8$^+$ T cells were labeled with 670 dye (BioLegend) and injected intravenously into B16-OVA-bearing mice.[22] Tumor growth was recorded every 3 days. Six mice per group were sacrificed on day 9 for functional analysis of infiltrated CD8$^+$ T cells. The remaining mice were continually monitored, and tumor growth was recorded until day 15. Lymph node and tumor tissues were obtained and digested as single cell suspensions for flow analysis.

Also, WT and GPR84 knockout mice were used to construct B16 or LLC models. The tumor volume and survival time were recorded. Tumor tissues were obtained for flow analysis or further pathological experiments.

Immunohistochemistry and immunofluorescence
Fresh tumor tissues were fixed in 4% paraformaldehyde for 48 hours at RT. Before embedding tissues into paraffin blocks, a graded ethanol series was used to dehydrate the tissues and replaced with xylene. Paraffin-embedded tissues were cut into 5 µm sections, deparaffinized with xylene, and rehydrated using a graded ethanol series. After quenching endogenous peroxidase by incubating the sections in 0.3% H$_2$O$_2$ for 30 min at RT, the tissues were blocked with 2% BSA for 1 hour at RT. Tissue sections were incubated with primary antibodies against CD8/IL-2/IFN-γ/TNF-α overnight at 4°C. Samples were then stained with an anti-rabbit antibody labeled with horseradish peroxidase. Images of the sections were randomly captured, and the number of CD8 T cells in each field was counted.

For immunofluorescence staining of cells, cells were fixed in 4% formaldehyde (CARLO ERBA Reagents) for 15 min, permeabilized in Triton-X 0.3% (Sigma) for 20 min, blocked for 1 hour at RT with 1% BSA, and stained with primary antibodies against GPR84 and γH2AX (Abcam) overnight at 4°C. The cells were then incubated with the appropriate fluorochrome-conjugated secondary antibodies for 1 hour at RT. Nuclei were counterstained with 4,6-diamino-2-phenylindole (DAPI), and slides were analyzed using fluorescence microscopy.

Telomeres length detection

CD8^{+} T cells were obtained for telomere length (ShangHai Biowing applied biotechnology) detection after co-cultured with WT or GPR84^{−/−} MDSCs-cultured supernatant. Briefly, T cells were centrifuged to get the pellet for DNA extraction. Then, samples were added into the qPCR mix. At the same time, different concentrations of standards were used. Construct a standard curve using the average CT value under 3 or 4 concentration gradients of the standard as the x-axis and the log2 concentration as the y-axis. Substitute the CT values of the sample's telomeres and internal reference channels into the standard curve equation to obtain the T/S of the sample.

RNA-sequencing and analysis

CD8^{+} T cells were cultured with WT or GPR84^{−/−} MDSCs-cultured supernatant for 2 days and stored in TRIzol at −80°C. The samples were sent to Sangon Biological for RNA-sequencing (RNA-seq). Gene differential expression analysis was performed using the Cuffdiff program in the Cufflinks package (https://github.com/cole-trap-nell-lab/cufflinks). The results were visualized using the R package ggplot2 using R Studio software. Gene set enrichment analysis (GSEA) was applied to the H (hallmark) gene sets.

Senescence-associated-beta-galactosidase staining and ROS detection

SA-β-gal activity in senescent CD8^{+} T cells was detected as previously described.[16] WT or Trp 53[−/−] CD8^{+} T cells were cultured with WT or GPR84^{−/−} MDSCs-cultured supernatant and then stained with SA-β-gal staining reagent (Beyotime).

Using the same culture conditions as above, CD8^{+} T cells were resuspended in 1 mL PBS mixed with the fluorescent probe 2,7-dichlorofluorescein diacetate (10 µmol/L) and incubated at 37°C for 30 min with inversion and mixing every 5 min. The presence of ROS (AAT Bioquest) was evaluated using fluorescein isothiocyanat (FITC) fluorescence and flow cytometry.

Clinical samples

Peripheral blood (3–4 mL) was collected from healthy donors and patients with tumors, whether receiving chemotherapy or not. Patients receiving chemotherapy were further divided into chemotherapy-sensitive and resistant. Peripheral blood mononuclear cells (PBMCs) were obtained by density-gradient centrifugation using a lymphocyte separation solution. MDSCs or CD8^{+} T cells were labeled with antibodies for flow cytometry. This study was approved by Ethics Committee of the First Affiliated Hospital of Zhengzhou University (approval 2019-KY-256).

Cell killing experiment

MDSCs were induced from WT or GPR84^{−/−} mice bone marrow. And CD8^{+} T cells were purified and activated from OT-1 mice. B16-OVA cells were co-cultured with MDSCs and CD8^{+} T cells (4:1). Fourty-eight hours later, the suspension cells were removed and B16-cells were digested for apoptosis analysis.

Antibodies and flow cytometry

Single cell suspensions were immune-stained with various combinations of fluorescent dye-conjugated antibodies against the following proteins: annexin V-Pacific Blue (Thermo), 7-AAD (BioLegend), Cell Proliferation Dye eFluor 670 (BioLegend), Anti-mouse CD3 (BioLegend; Clone17A2), Anti-mouse CD8a (BioLegend; 53–6.7), Anti-mouse IL-2 (BioLegend), Anti-mouse IFN-γ (BioLegend; XMG1.2), Anti-mouse TNF-α (BioLegend; MP6-XT22), Anti-mouse Ki67 (BioLegend; 16A8), Anti-mouse granzym B (BioLegend; QA16A02), Anti-mouse CD11B (BioLegend; M1/70), Anti-mouse Gr-1 (BioLegend; RB6-8C5), Anti-mouse CD27 (BioLegend; LG.3A10), Anti-mouse CD28 (BioLegend; 37.51), Anti-mouse 57 (Santa Cruz Biotechnology, sc-6261), Anti-mouse KLRG1 (BioLegend; 2F1), Anti-human CD3 (BioLegend; UCHT1), Anti-human CD8 (BioLegend; SK1), Anti-human CD15 (BioLegend; HI98), Anti-human CD14 (BioLegend; HCD14), Anti-human HLADR (BioLegend; L243), Anti-human CD11B (BioLegend; M1/70), Anti-human CD33 (BioLegend; P67.6), Anti-human IL-2 (BioLegend; MQ1-17H12), Anti-human TNF-α (BioLegend; Mab11), Anti-human IFN-γ (BioLegend; 4S.B3), and Anti mouse/human GPR84 (Bioss).

Statistical analysis

FlowJo software was used for the analysis of FACS data. Statistical analysis was conducted using GraphPad Prism software. For a single comparison between two groups, unpaired t-tests were used. Differences in survival were calculated using the Kaplan-Meier survival analysis. Data are presented as the mean±SEM or mean±SD. Spearman correlation analysis was used to evaluate the correlation.

RESULTS

Inhibition of cytotoxic CD8^{+} T cells by MDSCs depends on GPR84 transfer

We previously demonstrated that GPR84 aggravated the immunosuppressive function of MDSCs in both mice and human models.[6] The present study was designed to investigate the mechanisms of GPR84-strengthened MDSCs immunosuppression and the resultant suppression of CD8^{+} T cells. Herein, wild type and GPR84 knockout B6 mice were used for the in vitro investigation. The induction efficiency of GPR84 on MDSCs was examined at both protein (online supplemental figure S1A) and messenger RNA (mRNA) levels (online supplemental figure S1B). Consistent with the our group previous research,[6] we found that GPR84^{+} MDSCs inhibit the CD8^{+} T-cell anti-tumor response (figure 1A), proliferation (figure 1B), and cytotoxic function-related cytokine levels (figure 1C) to a greater degree than MDSCs lacking GPR84. We observed elevated GPR84 expression on CD8^{+} T cells after being co-cultured with GPR84^{+} MDSCs (figure 1D).
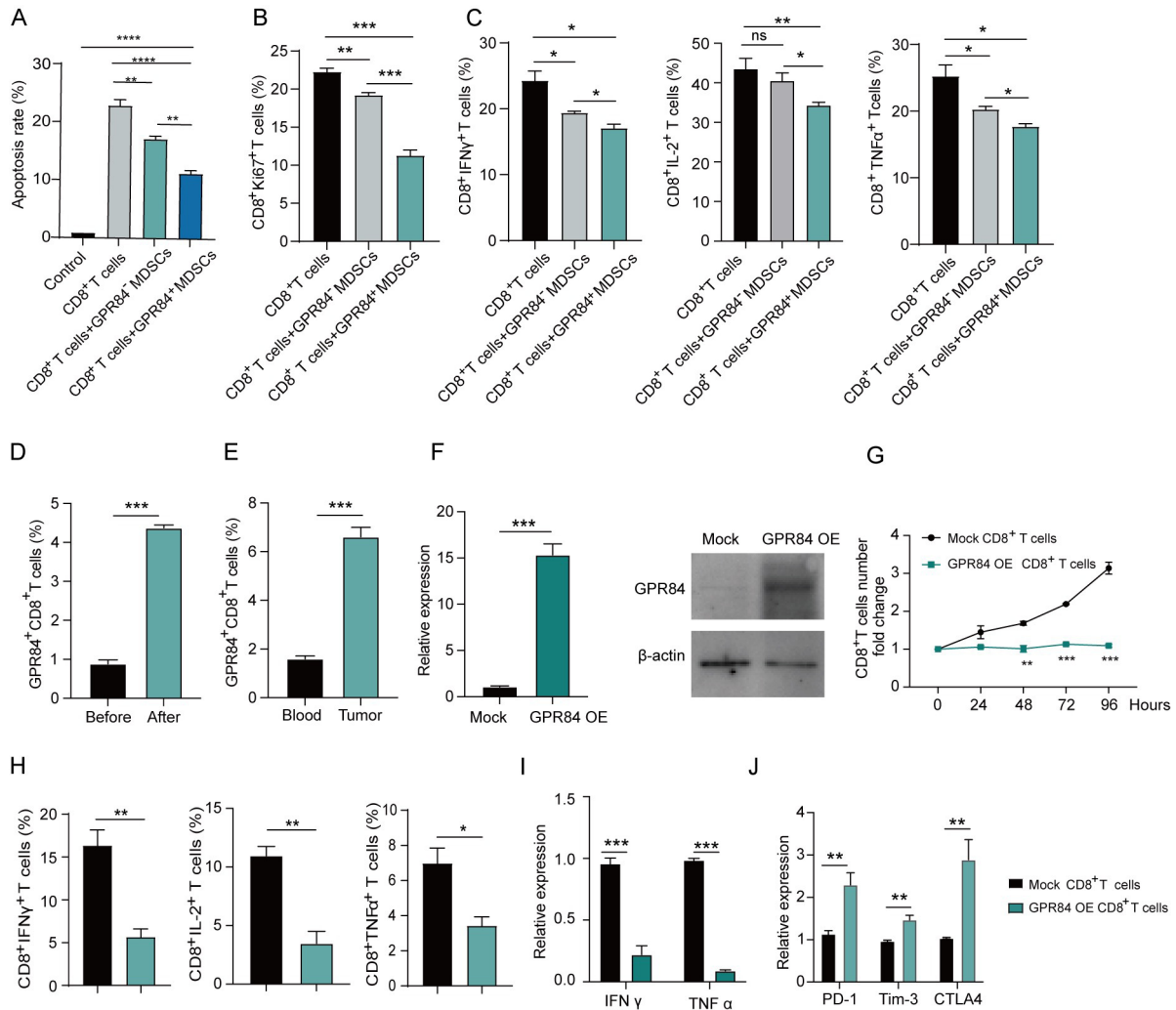
Figure 1 MDSCs inhibits CD8⁺ T-cell cytotoxicity depends on the GPR84 transfer. (A) The apoptotic rates of B16-OVA cells co-cultured with OT-I CD8⁺ T cells and GPR84⁺/⁻ MDSCs for 6 hours (CD8⁺ T cells: MDSCs: tumor cells=1:4:1). CD8⁺ T cells and GPR84⁺/⁻ MDSCs were co-cultured for 24 hours. Flow cytometry was used to analyze the proliferation (B) and function (C) of CD8⁺ T cells (CD8⁺ T cells: MDSCs=1:4). (D) The percentage of GPR84⁺ CD8⁺ T cells before and after being co-cultured with MDSCs (CD8⁺ T cells: MDSCs=1:4) was examined using flow cytometry. (E) The ratio of GPR84⁺ CD8⁺ T cells in blood and tumor tissues was detected in mice models bearing LLC cells. (F) CD8⁺ T cells were purified from C57 mice spleens after activation with an anti-CD3/CD28 antibody; the GPR84 plasmid was transfected, and GPR84-overexpressed CD8⁺ T cells were constructed. The transfection efficiency was examined using qRT-PCR and western blotting. Flow cytometry was used to analyze the proliferation (G) and function (H) of mock or GPR84-overexpressed CD8⁺ T cells. (I–J) The expression levels of functional and exhaustion-related genes on GPR84 overexpressed or mock CD8⁺ T cells were examined using qRT-PCR. Data were represented in at least three independent experiments. Data were presented as the mean±SEM. ns, not significant, *p<0.05, **p<0.01, ***p<0.001, ****p<0.0001. GPR84, G-protein-coupled receptor 84; MDSC, myeloid-derived suppressor cell; qRT-PCR, quantitative real-time PCR.

Additionally, a higher per cent of GPR84⁺CD8⁺ T cells was observed in tumor tissues than in paired peripheral blood (figure 1E), indicating the potential role of GPR84 in regulating CD8⁺ T cells function. We then transduced activated CD8⁺ T cells with the GPR84 plasmid and determined the antitumor response of GPR84 overexpression at both mRNA and protein levels (figure 1F and online supplemental figure 1). We evaluated the influence of GPR84 on CD8⁺ T-cell function and observed suppressed proliferation (figure 1G) and decreased cytotoxic function-related cytokine secretion in the GPR84-overexpressed group (figure 1H). Moreover, we observed

higher levels of exhaustion-related markers in GPR84-overexpressed CD8⁺ T cells (figure 1J). These results indicate that elevated GPR84 on CD8⁺ T cells after MDSCs co-culture may be responsible for the repressed anti-tumor ability.

Loss of GPR84 enhances the antitumor immunity of CD8⁺ T cells

Then, we constructed transgenic GPR84 knockout mice (online supplemental figure 1) and detected the function of CD8⁺ T cells. In contrast to the results observed in GPR84 overexpressed group, depleting GPR84 resulted
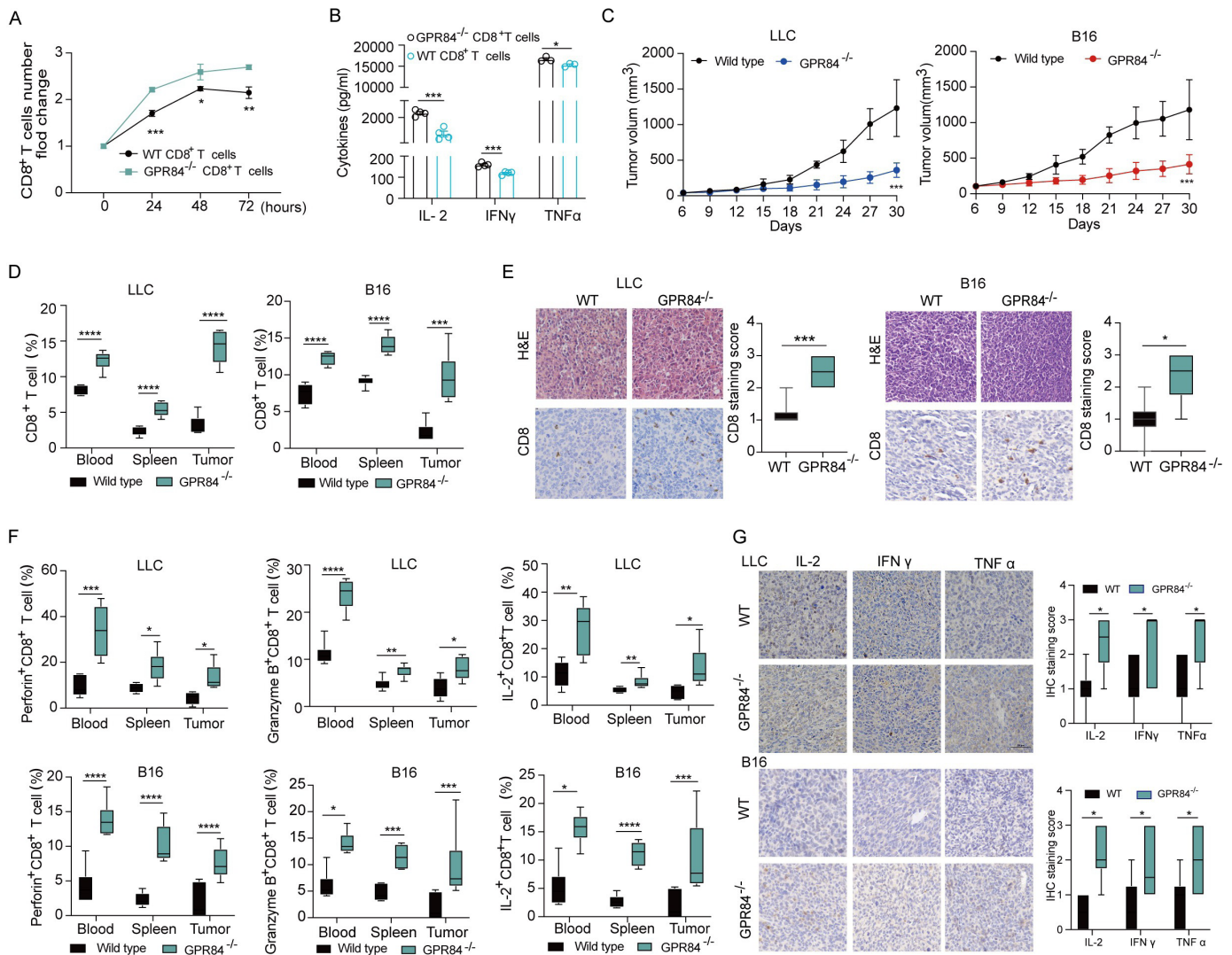
Figure 2 Loss of *GPR84* enhances antitumor immunity of CD8$^+$ T cells. GPR84, G-protein-coupled receptor 84; MDSC, myeloid-derived suppressor cell.

in the elevated ability to proliferate (figure 2A) and to secret functional cytokines in CD8$^+$ T cells (figure 2B). Moreover, we constructed mice models bearing LLC or B16 cells and observed that GPR84 depletion delayed the tumor growth (figure 2C). Flow cytometry examination exhibited higher CD8$^+$ T cells per cents in the blood, spleen and tumor sites from GPR84 knockout mice than those in the wild type mice (figure 2D) and immunohistochemistry (IHC) staining obtained similar results (figure 2E). Additionally, higher per cents of perforin, granzyme B and IL-2 positive CD8$^+$ T cells were observed in GPR84 knockout mice bearing LLC or B16 cells (figure 2F). Consistently, intensive CD8$^+$ T-cell infiltration to tumor sites and higher levels of functional cytokines (IL-2, IFN-γ, TNF-α) were observed in GPR84 knockout mice bearing LLC or B16 cells (figure 2G). Overall, these data indicate that GPR84 depletion release the suppressed function of CD8$^+$ T cells.

GPR84 suppressed the infiltration and reduced the antitumor ability of CD8$^+$ T cells

We went on to illustrate the role of GPR84 on CD8$^+$ T cells function in vivo. First, we generated GPR84$^{-/-}$ OT-1 mice by crossing GPR84$^{-/-}$ mice with OT-1 transgenic mice (online supplemental figure 1). To investigate the function of GPR84 in CD8$^+$ T cells, we transferred equal numbers of WT or GPR84$^{-/-}$ OT-I CD8$^+$ T cells into mice bearing B16-OVA cells and sacrificed them 15 days later (figure 3A). According to the results, GPR84$^{-/-}$ CD8$^+$ T cells exhibited a stronger ability to suppress tumor growth than OT-1 WT CD8$^+$ T cells (figure 3B and C). Additionally, GPR84$^{-/-}$ CD8$^+$ T cells exhibited elevated infiltration into the lymph nodes (figure 3D). Previous research has shown that CD8$^+$ T cells homing to tumor sites is critical for the antitumor immune response.[23] We observed a higher proportion of CD8$^+$ T cells in tumor tissues from GPR84$^{-/-}$ OT-1 mice than those from WT OT-1 mice (figure 3E and F). Furthermore, cytotoxic cytokines in
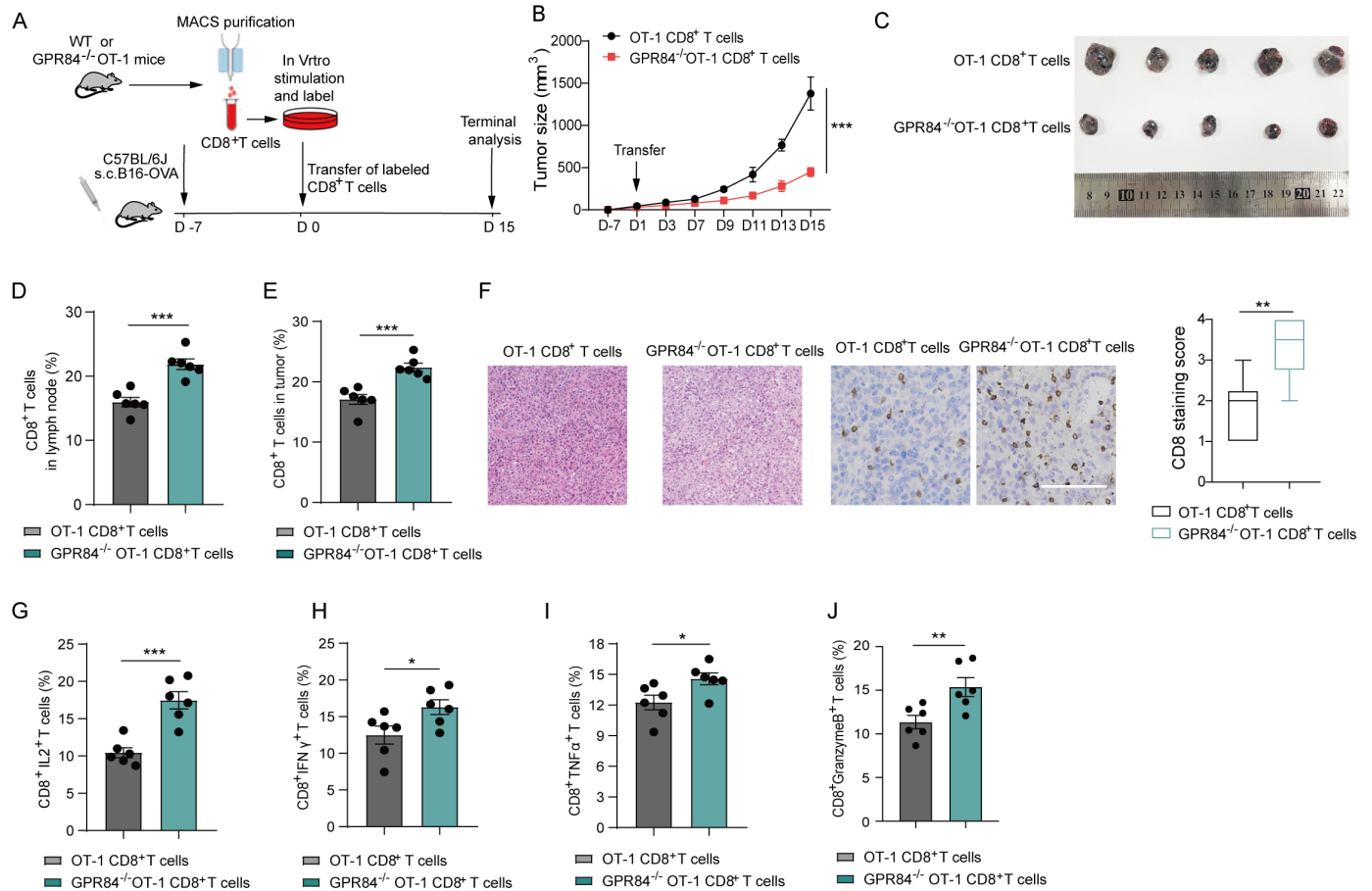
Figure 3 GPR84 suppresses the infiltration and reduces the antitumor ability of CD8^{+}T cells. GPR84, G-protein-coupled receptor 84; IFN, interferon; IL, interleukin; MACS, magnet-activated cell sorting; s.c., subcutaneous under the skin; WT, wild type.

CD8^{+} T cells in tumor tissues were significantly higher in infiltrated GPR84^{−/−} CD8^{+} T cells than in WT CD8^{+} T cells (figure 3G–J). These findings were consistent with those data of our former experiments (figures 1–2). Taken together, these results indicate that GPR84 suppressed the infiltration and function of CD8^{+} T cells in the TME, and the depletion of GPR84 liberated the suppression of CD8^{+} T cells.

MDSCs transfer GPR84 to CD8^{+} T cells in an exosome-dependent way to repress CD8^{+} T cells function

We showed that the transfer of GPR84 from MDSCs to CD8^{+} T cells contributes to aggregated immune suppression. We went on to investigate the mechanisms behind GPR84 translocation. First, we analyzed the mRNA levels of GPR84 on CD8^{+} T cells before and after co-culturing with MDSCs and observed no difference (figure 4A). Plus, when co-culturing CD8^{+} T cells (from the spleen of GPR84^{−/−} mice) with GPR84^{+} MDSCs, GPR84 expression was detected in CD8^{+} T cells (figure 4B and C), excluding the induction of GPR84 on CD8^{+} T cells by MDSCs. MDSCs interact with CD8^{+} T cells directly or indirectly to suppress the antitumor response.[24] We co-cultured CD8^{+} T cells with WT or GPR84^{−/−} MDSCs and observed higher levels of GPR84 on CD8^{+} T cells in the GPR84^{+} MDSCs

group than those in the GPR84^{−} MDSCs, both in cell contact (figure 4D) and non-contact systems (figure 4E). Additionally, CD8^{+} T cells treated with the cultured medium from WT or GPR84^{−/−} MDSCs achieved a similar trend (figure 4F), indicating that GPR84 transfer is independent of cell contact communication. No difference in GPR84 levels was observed in CD8^{+} T cells (mRNA level, figure 4A) and MDSCs (protein level, figure 4G) after co-culture. Collectively, these data demonstrate that GPR84 was transferred from MDSCs to CD8^{+} T cells; however, this action was not induced by MDSCs.

We then explored the mechanism of GPR84 translocation. Recent studies have shown that MDSCs suppress the CD8^{+} T cells antitumor response through PD-L1-containing-Exo secretion.[25] Based on the above data, we hypothesized that the Exo may be involved in this process. To test this, we applied the Exo-secreting inhibitor GW4869 and found that the per cent of GPR84^{+}CD8^{+} T cells was significantly reduced compared with that of the control group (figure 4H). This result suggests that the transfer of GPR84 may be dependent on MDSCs Exo secretion. We then isolated Exos from WT or GPR84^{−/−} MDSCs cultured supernatant and observed a vesicle-like morphology with a lipid bilayer structure and size
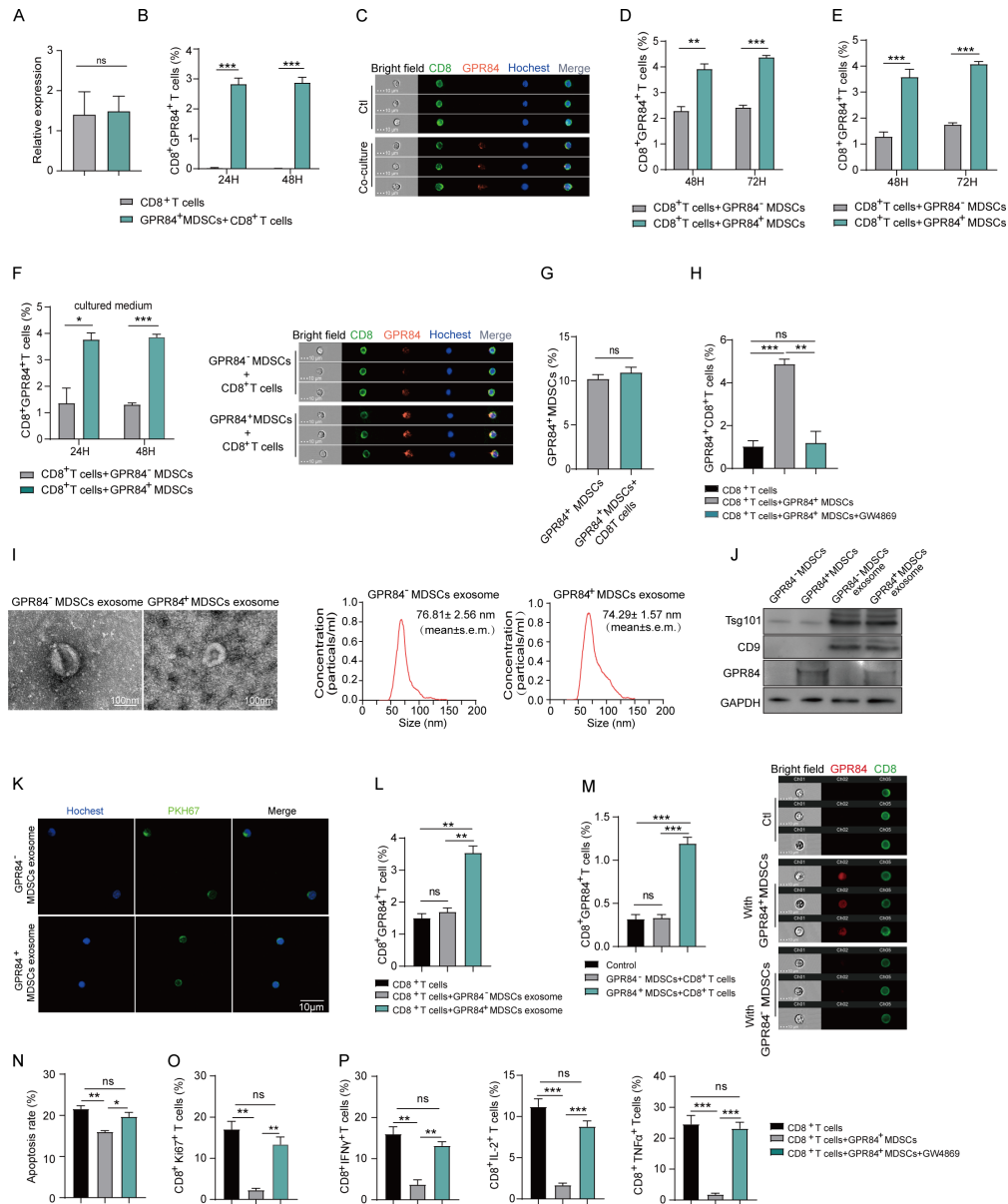
Figure 4 MDSCs transfer GPR84 to CD8^{+} T cells in an exosome-dependent way to repress CD8^{+} T-cell function. (A) After co-culturing with WT or GPR84^{-/-}MDSCs for 48 hours, the expression of GPR84 on CD8^{+} T cells was determined using quantitative real-time PCR (qRT-PCR). (B–C) CD8^{+} T cells were purified from GPR84-KO mice and co-cultured with GPR84^{+} MDSCs. Then, flow cytometry (B) and imaging flow cytometry (C) were used to analyze the expression of GPR84 on CD8^{+} T cells. (D–E) Co-cultured CD8^{+} T cells with WT or GPR84^{-/-} MDSCs directly (D) or indirectly (E). Flow cytometry was used to analyze the percentage of GPR84^{+}CD8^{+} T cells at 48 hours and 72 hours. (F) CD8^{+} T cells were cultured in the cultured supernatant of WT or GPR84^{-/-} MDSCs. Flow cytometry and imaging flow cytometry were used to analyze the expression of GPR84 on CD8^{+} T cells. (G) Flow cytometry was used to analyze the percentage of GPR84^{+} MDSCs after co-culturing with or without CD8^{+} T cells. (H) GPR84^{+} MDSCs were pretreated with GW4869 for 2 hours and then co-cultured with CD8^{+} T cells. After 48 hours, the percentage of GPR84^{+}CD8^{+} T cells was analyzed using flow cytometry. (I) The morphology of exosomes obtained from WT or GPR84^{-/-} MDSCs was detected using electron microscopy. The size distribution of the exosomes obtained from WT or GPR84^{-/-} MDSCs was measured by using NTA assay. (J) The expression levels of Tsg101, CD9, GPR84, and GAPDH in MDSCs and MDSC-derived exosomes were examined using western blotting. (K) Representative images of PKH-67 (green) on CD8^{+} T cells co-cultured for 24 hours with PKH-67-tagged MDSC-derived exosomes. Nucleus was counter-stained with Hoechst (blue). (Bar, 10 µm). (L) CD8^{+} T cells were co-cultured with WT or GPR84^{-/-} MDSCs-derived exosome for 24 hours. Flow cytometry was used to analyze the expression of GPR84 on CD8^{+} T cells. (M) CD8^{+} T cells were co-cultured with GPR84 antibody-tagged MDSCs for 24 hours. Then, flow cytometry was used to analyze the expression of GPR84 on CD8^{+} T cells. (N) GPR84^{+} MDSCs were pretreated with GW4869 for 2 hours and then co-cultured with CD8^{+} T cells. The killing ability (N) proliferation (O) and function-related cytokines (P) of CD8^{+} T cells were analyzed using flow cytometry. Data were represented in at least three independent experiments. Data were presented as the mean±SEM. ns, not significant, *p<0.05, **p<0.01, ***p<0.001, ****p<0.0001. GPR84, G-protein-coupled receptor 84; IFN, interferon; IL, interleukin; MDSC, myeloid-derived suppressor cell; NTA, nanoparticle tracking analysis; WT, wild type.

distribution (figure 4I). In addition, CD9 and Tsg101 were detected in isolated Exos (figure 4J). GPR84 was observed in the Exos of GPR84$^+$ MDSCs but not in those of GPR84$^-$ MDSCs (figure 4J), suggesting that MDSCs produced GPR84-containing Exo. We then investigated whether MDSCs-Exos could be taken up by CD8$^+$ T cells. PKH67 was used to label the Exos of WT or GPR84$^{-/-}$ MDSCs and then co-cultured with CD8$^+$ T cells. Fluorescence signaling was detected in CD8$^+$ T cells in both groups (figure 4K), confirming the absorption of MDSCs-Exos by CD8$^+$ T cells. When treating CD8$^+$ T cells with Exos from WT or GPR84$^{-/-}$ MDSCs, GPR84$^+$CD8$^+$ T cells had a higher percentage in the group treated with Exos from GPR84$^+$ MDSCs (figure 4L). Exos contribute to intercellular communication by transporting functionally active molecules, including proteins, micro-RNA, mRNA, single-stranded, and double-stranded DNA molecules.[26] No difference in GPR84 mRNA level was observed when CD8$^+$ T cells were co-cultured with or without GPR84$^+$ MDSCs (figure 4A). Additionally, MDSCs-Exos contained GPR84 protein (figure 4J), suggesting that GPR84 may be transformed from MDSCs to CD8$^+$ T cells in protein form. We, therefore, co-cultured CD8$^+$ T cells with GPR84 antibody-labeled MDSCs and detected the fluorescence signal on CD8$^+$ T cells (figure 4M). These results verified that the GPR84 was translocated MDSCs to CD8$^+$ T cells in the protein via the Exo manner. Finally, applying GW4869 to block the transfer of GPR84, we observed enhanced antitumor activity (figure 4N), stronger proliferation (figure 4O), and elevated levels of cytotoxic cytokine-related functions in CD8$^+$ T cells (figure 4P). Overall, these data demonstrate that GPR84 is transferred through the Exo in a protein form, causing GPR84 strengthened MDSCs-mediated suppression of CD8$^+$ T cells.

GPR84 induces the senescence of CD8$^+$ T cells via the p53 pathway

We went on to reveal the underlying mechanism of transferred GPR84 suppressed CD8$^+$ T cells function. RNA-seq was performed on CD8$^+$ T cells cultured with the supernatant from WT or GPR84$^{-/-}$ MDSCs to define the GPR84 transfer-induced transcriptomic differences. When analyzing the gene expression profiles between these groups using the principal component analysis (online supplemental figure 2), a strong transcriptional difference was observed. Furthermore, significantly downregulated and upregulated genes were identified (online supplemental figure 2). Heatmaps were used to identify the hierarchical clustering of the gene expression matrix (online supplemental figure 2). Gene Ontology and Kyoto Encyclopedia of Genes and Genomes (KEGG) enrichment analyses identified that cell cycle-related pathways, including DNA replication and p53 signaling pathways, were elevated in CD8$^+$ T cells cultured with the supernatant from GPR84$^+$ MDSCs (figure 5A and online supplemental figure 2). Moreover, the GSEA showed that the p53 signaling pathway was enriched (figure 5B) and that p53 pathway-related genes were upregulated

(figure 5C) in CD8$^+$ T cells cultured with the supernatant from GPR84$^+$ MDSCs. Further, we verified the enriched p53 signaling in CD8$^+$ T cells after being treated with supernatant from GPR84$^+$ MDSCs both in mRNA (figure 5D) and protein (figure 5E) levels. These results indicate that GPR84 transferred from MDSCs activate the p53 signaling pathway in CD8$^+$ T cells.

The activation of p53 in T cells induces the senescence-like phenotype to suppress T-cell function.[16] Therefore, we explored whether transferred GPR84 induces the senescence of CD8$^+$ T cells by using SA-β-gal staining. CD8$^+$ T cells co-cultured with GPR84$^+$ MDSCs supernatant showed significantly higher SA-β-gal positive cell numbers (figure 5F). Senescent T cells were also characterized as CD27/CD28 negative, and CD57/KLRG1 positive.[21] Here, we observed higher per cent of CD27$^-$/CD28$^-$/CD57$^+$/KLRG1$^+$ in CD8$^+$ T cells co-cultured with GPR84$^+$ MDSCs (figure 5G). To verify the involvement of p53 in GPR84 transferred induced CD8$^+$ T cells senescence, we purchased Trp53$^{-/-}$ mice. Then, we co-cultured Trp53$^{-/-}$ or WT CD8$^+$ T cells with the supernatant from WT MDSCs. Forty-eight hours later, we examined the SA-β-gal staining and CD27/CD28/KLRG1/CD57 levels. Co-cultured with GPR84$^+$ MDSCs supernatant induced higher per cent of CD27$^-$/CD28$^-$/CD57$^+$/KLRG1$^+$ and SA-β-gal positive in wild type CD8$^+$ T cells, while the phenomenon was not observed in the Trp53$^{-/-}$ CD8$^+$ T cells (figure 5H and I), indicating that GPR84 transferred to CD8$^+$ T cells induced T cells senescence depending on the p53 signaling. The p53 pathway may induce T-cell senescence by activating DNA damage.[27] We then considered whether DNA damage was involved in GPR84-induced CD8$^+$ T-cell senescence. The histone protein H2AX at residue S139 (γH2AX) has been regarded as the marker of DNA damage. Herein, we obtained the supernatant from GPR84$^+$ and GPR84$^-$ MDSCs and then co-cultured with CD8$^+$ T cells. After 48 hours, CD8$^+$ T cells were used for γH2AX staining and we observed higher γH2AX level in the supernatant from GPR84$^+$ MDSCs than in the supernatant from GPR84$^-$ MDSCs (figure 5J). Plus, telomere length, a marker of senescence,[28] was shorter in CD8$^+$ T cells cultured after the supernatant from GPR84$^+$ MDSCs (figure 5K), indicating that GPR84 transferred from MDSCs induced DNA damage and senescence in CD8$^+$ T cells. Excess ROS induces DNA damage, which further suppresses T cells function and induces cell death.[29] To test whether ROS was the reason for p53-mediated DNA damage that induced CD8$^+$ T-cell senescence, we analyzed ROS production in CD8$^+$ T cells co-cultured with GPR84$^{+/-}$ MDSCs. CD8$^+$ T cells co-cultured with GPR84$^+$ MDSCs produced high levels of ROS (figure 5L). These results demonstrate that the transfer of GPR84 to CD8$^+$ T cells induces T-cell senescence, mediated by the p53 regulated ROS-DNA damage pathway.

The clinical significance of GPR84 levels in CD8$^+$ T cells

We evaluated the clinical significance of GPR84$^+$ CD8$^+$ T cells. Using the data from The Cancer Genome Atlas
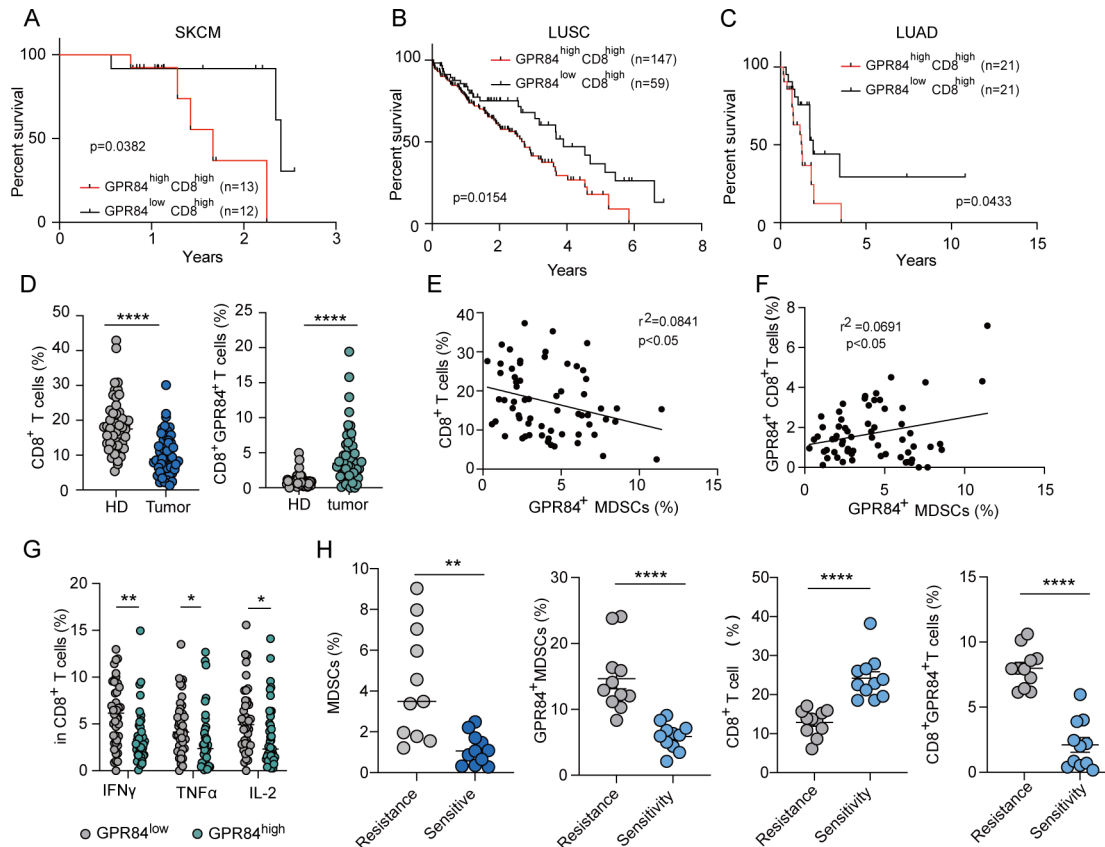
Figure 5 GPR84 induces the senescence of CD8+ T cells via the p53 pathway. CM, cultured medium; DAPI, 4,6-diamino-2-phenyl indole; GPR84, G-protein-coupled receptor 84; KEGG, Kyoto Encyclopedia of Genes and Genomes; MDSC, myeloid-derived suppressor cell; ROS, reactive oxygen species.

(TCGA), we subgrouped patients with skin cutaneous melanoma, lung adenocarcinoma (LUAD), and lung squamous cell cancer (LUSC) with high and low CD8 infiltration depending on GPR84 expression in the tumor sites. The Kaplan-Meier survival analysis revealed that patients with GPR84lowCD8high had better survival rates compared with those patients with GPR84highCD8high (figure 6A–C). Moreover, we collected PBMCs from patients with tumor and healthy donors and examined the per cent of GPR84+CD8+ T cells. We observed a lower per cent of CD8+ T cells, while a higher percentage of GPR84+CD8+ T cells in patients with tumor (figure 6D). Furthermore, we examined the immune cells per cents in healthy cohort and observed a negative correlation

between GPR84+ MDSCs and CD8+ T cells (figure 6E), while a positive correlation was observed between GPR84+CD8+ T cells and GPR84+ MDSCs (figure 6F). Additionally, we compared the function of CD8+ T cells with high and low expression of GPR84 and observed a lower percentage of IL-2/IFN-γ/TNF-α in CD8+ T cells with higher GPR84 levels (figure 6G). These results were consistent with the conclusion in figures 3–4, suggesting suppressed CD8+ T-cell function by GPR84.

Though regarded as the classic traditional cancer therapy, chemotherapy has also been reported to elevate the MDSCs accumulation to promote cancer progression.[30] Correspondingly, MDSCs induced chemo-resistance through exosomal-mediated mechanism.[31]

Figure 6 Clinical significance of GPR84 levels in CD8⁺ T cells. (A–C) Overall survival of skin cutaneous melanoma (SKCM), lung adenocarcinoma (LUAD), and lung squamous cell cancer (LUSC) was analyzed in GPR84^{high} CD8^{high} and GPR84^{low} CD8^{high} groups based on the data from The Cancer Genome Atlas. (D) The percentage of CD8⁺ T and GPR84⁺ CD8⁺ T cells in peripheral blood mononuclear cells from healthy donors (n=50) and patients with cancer (n=50) was analyzed using flow cytometry. (E) The correlation between CD8⁺ T cells and GPR84⁺ MDSCs was analyzed based on the flow cytometry data from healthy donors (n=63). (F) The correlation between GPR84⁺ CD8⁺ T cells and GPR84⁺ MDSCs was analyzed based on the flow cytometry data from healthy donors (n=63). (G) The expression of function-related markers in GPR84^{high} and GPR84^{low} CD8⁺ T cells was analyzed using flow cytometry from healthy donors (n=63). (H) The percentages of MDSCs, GPR84⁺ MDSCs, CD8⁺ T cells, and GPR84⁺ CD8⁺ T cells were analyzed in chemotherapy-resistant (n=11) or sensitive (n=11) patients with cancer using flow cytometry. Data were represented in at least three independent experiments. Data were presented as the mean±SEM. ns, not significant, *p<0.05, **p<0.01, ***p<0.001, ****p<0.0001. GPR84, G-protein-coupled receptor 84; HD, healthy donor; IFN, interferon; IL, interleukin; MDSC, myeloid-derived suppressor cell; TNF, tumor necrosis factor.

Our previously reported study convinced the correlation between GPR84⁺ MDSCs and anti-PD-1 therapy failure.[6] Herein, we tried to reveal whether GPR84 was associated with chemo-resistance. We analyzed GPR84 expression in CD8⁺ T cells and MDSCs from patients with cancer who were sensitive or resistant to chemotherapy and observed higher levels of GPR84⁺CD8⁺ T cells in patients resistant to chemotherapy (figure 6H). These results indicate that GPR84⁺CD8⁺ T cells may work as an indicator to predict a patient's response to chemotherapy. Furthermore, blocking GPR84 may reverse chemoresistance by eliminating GPR84⁺ MDSCs and restoring the antitumor response of GPR84⁺ CD8⁺ T cells.

DISCUSSION

As revealed by reported studies, tumor progression and treatment efficacy can be influenced by the interaction between MDSCs and CD8⁺ T cells in the TME.[32 33] Further,

it has been proved that the accumulation of MDSCs exhibited stronger immunosuppression to CD8⁺ T cells to attenuate the antitumor response, and eliminating MDSCs suppressed tumor progression and enhanced immunotherapy efficacy.[20] Until now, no approved therapeutic agents that specifically target MDSCs have been applied in clinical practise due to the limited identified markers on MDSCs. Previously, we revealed that GPR84 strengthened the immunosuppression of MDSCs to weaken CD8⁺ T cells function, and target blocking GPR84 enhanced the anti-PD-1 therapy efficacy.[6] However, the former study did not explore the alteration and underlying mechanism in CD8⁺ T cells that are induced by GPR84⁺ MDSCs. Therefore, we go on to perform this study as a series of research to explain the stronger immunosuppression endowed by GPR84 to MDSCs from the CD8⁺ T cells aspect. Herein, we observed the consistent phenomenon that GPR84⁺ MDSCs elicited enhanced immunosuppression to CD8⁺

T cells function both in vitro and in vivo. The transferred GPR84 from MDSCs to CD^{+}8 T cells explained the stronger inhibition of GPR84^{+} MDSCs. This effect was limited when using GPR84 knockout MDSCs. Mechanistically, GPR84-containing Exos secreted by MDSCs could be taken up by CD8^{+} T cells and induced DNA damage to cause T cells senescence in the p53 pathway.

As a pro-inflammatory orphan GPCR, GPR84 has been widely reported in immune cells, including monocytes, macrophages, and neutrophils,[34] and contributes to several inflammatory and fibrotic diseases.[35] Recently, several studies also revealed the role of GPR84 in cancer, including GPR84 mediates macrophage phagocytosis,[36 37] leukemia stem-cell proliferation.[38] Until now, no study revealed the role of GPR84 on neutrophils or T cells in the TME. Our group first reported the regulatory role of GPR84 on MDSCs,[6] herein, we observed that CD8^{+} T cells co-cultured with GPR84^{+} MDSCs exhibited suppressed antitumor ability, while knockout GPR84 reversed the phenomenon in the TME. The only reported study on GPR84 related to T cells was conducted by Venkataraman and Kuo.[39] Contrast to our findings, they found that GPR84 deficiency did not change the proliferation of T cells.[39] These conflicting results may be attributed to several differences between the aforementioned study and ours: (1) different T-cell populations; (2) distinctive manners to stimulate T cells; and (3) different research models.

We have convinced the negative regulation of transferred GPR84 from MDSCs to CD8^{+} T cells independent of cell–cell contact. Multiple studies have regarded Exos as an ideal cargo to convey functional components for the local and distal intercellular communication in the TME.[26] MDSCs-shed Exos contain bioactive proteins[40] and play essential roles in suppressing CD8^{+} T cells function.[25] Herein, when applying GW4869, an Exo release inhibitor, the transfer of GPR84 from MDSCs to CD8^{+} T cells diminished and the antitumor response was not suppressed in CD8^{+} T cells. Apart from MDSCs, other GPR84 expressed myeloid cells[41] can also secrete Exo in the TME.[42 43] This arises the hypothesis that GPR84 transferred to CD8^{+} T cells may not only from MDSCs but from macrophages and neutrophil. However, no studies have been reported to reveal the regulation of GPR84 on neutrophils function in the TME. Moreover, GPR84 has been identified as the contributor to macrophages phagocytosis of cancer cell,[36 37] while we convinced the negative modulation of transferred GPR84 to CD8^{+} T cells function. Therefore, whether GPR84 could be transformed by macrophages and neutrophil in the Exo manner and the following modulation on CD8^{+} T cells function need deep investigations.

Further, we identified an enriched p53 pathway in CD8^{+} T cells treated with GPR84^{+} MDSCs supernatant. p53 plays a key role in inducing cell cycle arrest, senescence, and apoptosis in response to aberrant oncogene activation or DNA damage.[27] A few studies have also demonstrated the critical role of p53 in T-cell senescence.[17] Herein,

we observed higher per cent of senescent CD8^{+} T cells in GPR84^{+} MDSCs. DNA damage is often regarded as a key factor in activating the p53 pathway.[44] Consistently, we found that DNA damage was severe in CD8^{+} T cells co-cultured with GPR84^{+} MDSCs. Peters *et al* reported that GPR84 induces Gα-dependent ERK activation, increases intracellular Ca and IP levels, and increases ROS production to mediate pro-inflammatory signaling in human macrophages.[45] The overproduction of ROS is responsible for DNA damage.[46] We observed higher ROS production in CD8^{+} T cells treated with GPR84^{+} MDSCs. Several studies have shown that ROS production occurs in response to the activation of multiple cellular receptors, including the transforming growth factor-β and insulin receptors.[47] In these cases, ROS acts as a secondary messenger that is necessary for protein kinases to activate gene expression and proliferation.[48] However, abnormal ROS production can adversely affect T cells. Excessive ROS production can induce cell apoptosis, resulting in blocked cell function and proliferation.[49] These findings are consistent with the hypothesis that the transfer of GPR84 from MDSCs to CD8^{+} T cells promotes ROS overproduction, which induces DNA damage, ultimately leading to the activation of p53 and cell senescence.

Also, transferred GPR84 may mediate the T-cell function beyond the induction of cellular senescence. GPR84, as a member of the GPCR superfamily, is a receptor for medium-chain fatty acids.[34] Some fatty acid receptors, responsible for fatty acid recognition and transmembrane transport between cells, can help cells absorb fatty acids from their surroundings.[50 51] However, abnormal fatty acid uptake can adversely affect the T-cell antitumor response.[52] The fatty acid receptor CD36 mediates tumor infiltration of CD8^{+} T cells to ingest fatty acids, causing lipid peroxidation and iron death, resulting in reduced cytotoxic factor production and an impaired antitumor ability.[53] In addition, over-ingested fatty acids damage the mitochondria, causing cell paralysis.[54] Though not investigated here, we presumed that transferred GPR84 may exacerbate the fatty acid uptake of CD8^{+} T cells, resulting in T-cell dysfunction. However, this point needs to be further studied from the perspective of metabolism in future.

The findings presented here established that GPR84 transfer from MDSCs to CD8^{+} T cells depends on Exo secretion. Furthermore, GPR84 transfer suppressed the antitumor ability of CD8^{+} T cells. Various studies have shown that extensive cytotoxic T-cell infiltration in the TME correlates with better prognosis.[15 55] However, here we found that patients with malignant melanoma, LUAD, and LUSC (TCGA data) with a GPR84^{high}CD8^{high} profile had a reduced survival period, implying that more accurate T-cell markers are necessary to predict the clinical prognosis. Previous studies have correlated the accumulation of MDSCs in the TME with the tolerance of patients to chemotherapy.[56] Consistent with these studies, we convinced the immunosuppression of MDSCs on CD8^{+} T cells through GPR84 translocation and its negative role in

the chemotherapeutic response. This result implies that the expression of GPR84 on CD8^{+} T cells may have therapeutic implications for chemotherapy.

In summary, our study shows that MDSCs can transfer GPR84 to CD8^{+} T cells by secreting Exos to induce excess ROS production in CD8^{+} T cells, leading to endogenous DNA damage, which in turn activates the p53 signaling pathway, causes CD8^{+} T-cell senescence, and ultimately inhibits the proliferation and function of CD8^{+} T cells. These results, in combination with the clinical sample analysis, suggest that GPR84 may be a promising target for relieving immunosuppression and enhancing the efficacy of immunotherapy and chemotherapy.

Competing interests No, there are no competing interests.

Patient consent for publication Not applicable.

Provenance and peer review Not commissioned; externally peer reviewed.

Data availability statement Data are available upon reasonable request.

ORCID iDs
Feng Li http://orcid.org/0000-0002-3895-0437
Yi Zhang http://orcid.org/0000-0001-9861-4681

REFERENCES

1 Kim W, Chu TH, Nienhüser H, *et al*. PD-1 signaling promotes tumor-infiltrating myeloid-derived Suppressor cells and gastric tumorigenesis in mice. *Gastroenterology* 2021;160:781–96.
2 Myeloid-derived Itaconate suppresses antitumor immunity. *Cancer Discov* 2022:OF1.
3 Halaby MJ, Hezaveh K, Lamorte S, *et al*. GCN2 drives macrophage and MDSC function and immunosuppression in the tumor microenvironment. *Sci Immunol* 2019;4:eaax8189.
4 Mohammadpour H, MacDonald CR, McCarthy PL, *et al*. 2-adrenergic receptor signaling regulates metabolic pathways critical to myeloid-derived suppressor cell function within the TME. *Cell Rep* 2021;37:109883.
5 Ajith A, Mamouni K, Horuzsko DD, *et al*. Targeting TREM1 augments antitumor T cell immunity by inhibiting myeloid-derived suppressor cells and restraining anti-PD-1 resistance. *J Clin Invest* 2023;133:e167951.
6 Qin G, Liu S, Liu J, *et al*. Overcoming resistance to immunotherapy by targeting GPR84 in myeloid-derived suppressor cells. *Signal Transduct Target Ther* 2023;8:164.
7 Pallett LJ, Swadling L, Diniz M, *et al*. Tissue CD14CD8 T cells reprogrammed by myeloid cells and modulated by LPS. *Nature* 2023;614:334–42.
8 De Cicco P, Ercolano G, Ianaro A. The new era of cancer immunotherapy: targeting myeloid-derived suppressor cells to overcome immune evasion. *Front Immunol* 2020;11:1680.
9 Gao X, Sui H, Zhao S, *et al*. Immunotherapy targeting myeloid-derived Suppressor cells (MDSCs) in tumor microenvironment. *Front Immunol* 2020;11:585214.
10 Kim R, Hashimoto A, Markosyan N, *et al*. Ferroptosis of tumour neutrophils causes immune suppression in cancer. *Nature* 2022;612:338–46.
11 Rashid MH, Borin TF, Ara R, *et al*. Critical immunosuppressive effect of MDSC-derived exosomes in the tumor microenvironment. *Oncol Rep* 2021;45:1171–81.
12 Ding X-Q, Wang Z-Y, Xia D, *et al*. Proteomic profiling of serum exosomes from patients with metastatic gastric cancer. *Front Oncol* 2020;10:1113.
13 Wang Y, Ding Y, Guo N, *et al*. MDSCs: key criminals of tumor pre-metastatic niche formation. *Front Immunol* 2019;10:172.
14 Qin G, Liu J, Lian J, *et al*. PMN-MDSCs-induced accumulation of CD8+CD39+ T cells predicts the efficacy of chemotherapy in esophageal squamous cell carcinoma. *Clin Transl Med* 2020;10:e232.
15 Ma S, Sun B, Duan S, *et al*. YTHDF2 Orchestrates tumor-associated macrophage reprogramming and controls antitumor immunity through CD8+ T cells. *Nat Immunol* 2023;24:255–66.
16 Legscha KJ, Antunes Ferreira E, Chamoun A, *et al*. Δ133P53A enhances metabolic and cellular fitness of TCR-engineered T cells and promotes superior antitumor immunity. *J Immunother Cancer* 2021;9:e001846.
17 Liu X, Hartman CL, Li L, *et al*. Reprogramming lipid metabolism prevents effector T cell senescence and enhances tumor Immunotherapy. *Sci Transl Med* 2021;13:eaaz6314.
18 Amin OE, Colbeck EJ, Daffis S, *et al*. Therapeutic potential of TLR8 agonist GS-9688 (selgantolimod) in chronic hepatitis B: remodeling of antiviral and regulatory mediators. *Hepatology* 2021;74:55–71.
19 Kishton RJ, Sukumar M, Restifo NP. Metabolic regulation of T cell longevity and function in tumor immunotherapy. *Cell Metab* 2017;26:94–109.
20 Veglia F, Sanseviero E, Gabrilovich DI. Myeloid-derived suppressor cells in the era of increasing myeloid cell diversity. *Nat Rev Immunol* 2021;21:485–98.
21 Chen H-A, Ho Y-J, Mezzadra R, *et al*. Senescence rewires microenvironment sensing to facilitate antitumor immunity. *Cancer Discov* 2023;13:432–53.
22 Sivan A, Corrales L, Hubert N, *et al*. Commensal bifidobacterium promotes antitumor immunity and facilitates anti-PD-L1 efficacy. *Science* 2015;350:1084–9.
23 Ping Y, Shan J, Liu Y, *et al*. Taurine enhances the antitumor efficacy of PD-1 antibody by boosting CD8(+) T cell function. *Cancer Immunol Immunother* 2023;72:1015–27.
24 Hegde S, Leader AM, Merad M. MDSC: markers, development, states, and unaddressed complexity. *Immunity* 2021;54:875–84.
25 Sun Y, Guo J, Yu L, *et al*. PD-L1(+) Exosomes from bone marrow-derived cells of tumor-bearing mice inhibit antitumor immunity. *Cell Mol Immunol* 2021;18:2402–9.
26 Zhou Z, Bonds MM, Edil BH, *et al*. Lysosomes promote cancer metastasis via exosome in PTEN-deficient tumors. *Gastroenterology* 2023;164:329–31.
27 Cartwright ANR, Suo S, Badrinath S, *et al*. Immunosuppressive myeloid cells induce nitric oxide-dependent DNA damage and P53 pathway activation in CD8(+) T cells. *Cancer Immunol Res* 2021;9:470–85.
28 Chakravarti D, LaBella KA, DePinho RA. Telomeres: history, health, and hallmarks of aging. *Cell* 2021;184:306–22.

29 Karl F, Liang C, Böttcher-Loschinski R, *et al*. Oxidative DNA damage in reconstituting T-cells is associated with relapse and inferior survival following Allo-SCT. *Blood* 2023;141:1626–39.

30 Monteran L, Ershaid N, Doron H, *et al*. Chemotherapy-induced complement signaling modulates immunosuppression and metastatic relapse in breast cancer. *Nat Commun* 2022;13:5797.

31 Deng Z, Rong Y, Teng Y, *et al*. Exosomes miR-126A released from MDSC induced by DOX treatment promotes lung metastasis. *Oncogene* 2017;36:639–51.

32 Jou E, Rodriguez-Rodriguez N, Ferreira A-C, *et al*. An innate IL-25-ILC2-MDSC axis creates a cancer-permissive Microenvironment for *Apc* mutation-driven intestinal tumorigenesis. *Sci Immunol* 2022;7:eabn0175.

33 Grover A, Sanseviero E, Timosenko E, *et al*. Myeloid-derived suppressor cells: a propitious road to clinic. *Cancer Discov* 2021;11:2693–706.

34 Wang J, Wu X, Simonavicius N, *et al*. Medium-chain fatty acids as ligands for orphan G protein-coupled receptor GPR84. *J Biol Chem* 2006;281:34457–64.

35 Zhang Q, Chen L-H, Yang H, *et al*. GPR84 signaling promotes intestinal mucosal inflammation via enhancing NLRP3 Inflammasome activation in macrophages. *Acta Pharmacol Sin* 2022;43:2042–54.

36 Kamber RA, Nishiga Y, Morton B, *et al*. Inter-cellular CRISPR screens reveal regulators of cancer cell phagocytosis. *Nature* 2021;597:549–54.

37 Zhang X, Wang Y, Supekar S, *et al*. Pro-phagocytic function and structural basis of GPR84 signaling. *Nat Commun* 2023;14:5706.

38 Dietrich PA, Yang C, Leung HHL, *et al*. GPR84 sustains aberrant β-catenin signaling in leukemic stem cells for maintenance of MLL leukemogenesis. *Blood* 2014;124:3284–94.

39 Venkataraman C, Kuo F. The G-protein coupled receptor, GPR84 regulates IL-4 production by T lymphocytes in response to CD3 crosslinking. *Immunol Lett* 2005;101:144–53.

40 Burke M, Choksawangkarn W, Edwards N, *et al*. Exosomes from myeloid-derived suppressor cells carry biologically active proteins. *J Proteome Res* 2014;13:836–43.

41 Liang T, Zhang B, Xing Z, *et al*. Adapting and remolding: orchestrating tumor microenvironment normalization with photodynamic therapy by size transformable nanoframeworks. *Angew Chem Int Ed Engl* 2021;60:11464–73. 10.1002/anie.202102180 Available: https://onlinelibrary.wiley.com/toc/15213773/60/20

42 Pu J, Xu Z, Nian J, *et al*. M2 macrophage-derived extracellular Vesicles facilitate CD8+T cell exhaustion in hepatocellular carcinoma via the miR-21-5p/YOD1/YAP/β-catenin pathway. *Cell Death Discov* 2021;7:182.

43 Zhang J, Ji C, Zhang H, *et al*. Engineered neutrophil-derived exosome-like Vesicles for targeted cancer therapy. *Sci Adv* 2022;8:eabj8207.

44 Mondal AM, Horikawa I, Pine SR, *et al*. p53 isoforms regulate aging- and tumor-associated replicative senescence in T lymphocytes. *J Clin Invest* 2013;123:70355:5247–57.:.

45 Peters A, Rabe P, Liebing A-D, *et al*. Hydroxycarboxylic acid receptor 3 and GPR84 - two metabolite-sensing G protein-coupled receptors with opposing functions in innate immune cells. *Pharmacol Res* 2022;176:106047.

46 Liu J, Zhang Y. Intratumor microbiome in cancer progression: current developments, challenges and future trends. *Biomark Res* 2022;10:37.

47 Koch RE, Josefson CC, Hill GE. Mitochondrial function, ornamentation, and immunocompetence. *Biol Rev Camb Philos Soc* 2017;92:1459–74.

48 Sena LA, Li S, Jairaman A, *et al*. Mitochondria are required for antigen-specific T cell activation through reactive oxygen species signaling. *Immunity* 2013;38:225–36.

49 Wang X, Zha H, Wu W, *et al*. CD200+ cytotoxic T lymphocytes in the tumor microenvironment are crucial for efficacious anti-PD-1/PD-L1 therapy. *Sci Transl Med* 2023;15:eabn5029.

50 Akasaka H, Tanaka T, Sano FK, *et al*. Structure of the active G-coupled human lysophosphatidic acid receptor 1 complexed with a potent agonist. *Nat Commun* 2022;13:5417.

51 Xiong Y, Ke R, Zhang Q, *et al*. Small activating RNA modulation of the G protein-coupled receptor for cancer treatment. *Adv Sci (Weinh)* 2022;9:2200562. 10.1002/advs.202200562 Available: https://onlinelibrary.wiley.com/toc/21983844/9/26

52 Corn KC, Windham MA, Rafat M. Lipids in the tumor microenvironment: from cancer progression to treatment. *Prog Lipid Res* 2020;80:101055.

53 Ma X, Xiao L, Liu L, *et al*. CD36-mediated ferroptosis dampens Intratumoral CD8+ T cell effector function and impairs their antitumor ability. *Cell Metab* 2021;33:1001–12.

54 Turkieh A, Caubère C, Barutaut M, *et al*. Apolipoprotein O is mitochondrial and promotes Lipotoxicity in heart. *J Clin Invest* 2014;124:2277–86.

55 Danlos F, Texier M, Job B, *et al*. Genomic instability and pro-tumoral inflammation are associated with primary resistance to anti-PD1 + anti-angiogenesis in malignant pleural mesothelioma. *Cancer* 2023.

56 Li C, You X, Xu X, *et al*. A metabolic reprogramming amino acid polymer as an immunosurveillance activator and leukemia targeting drug carrier for T-cell acute lymphoblastic leukemia. *Adv Sci (Weinh)* 2022;9:2104134.